Impact of carbonization on oak wood $\delta^{18}O$: a preliminary study

du Boisgueheneuc D.[1,3*], Delarue F.[2*], Daux V.[1], Nguyen Tu T.T.[2], Baudin F[4]., Dufraisse A.[3]

[1] *Laboratoire des Sciences du Climat et de l'Environnement/IPSL, UMR CEA/CNRS 1572, L'Orme des Merisiers, Bât. 701, CEA Saclay, 91191 Gif/Yvette Cedex, France*

[2] *Sorbonne Université, CNRS, EPHE, PSL, UMR 7619 METIS, 4 place Jussieu, 75005, Paris France*

[3] *UMR 7209 – AASPE- CNRS/MNHN, CP56, 55 rue Buffon, 75 005 Paris, France*

[4]*Sorbonne Université, CNRS, UMR 7193 ISTeP, 4 place Jussieu 75005 Paris, France*

* Corresponding authors at: Laboratoire des Sciences du Climat et de l'Environnement/IPSL, UMR CEA/CNRS 1572, L'Orme des Merisiers, Bât. 701, CEA Saclay, 91191 Gif/Yvette Cedex, France. E-mail address: diane.duboisgueheneuc@lsce.ipsl.fr (D. du Boisgueheneuc) ; *Sorbonne Université, CNRS, EPHE, PSL, UMR 7619 METIS, 4 place Jussieu, 75005, Paris France.* E-mail address: frederic.delarue@upmc.fr (F. Delarue)

Abstract:

The carbonization process induces significant physical, elemental, and structural transformations of wood. In this study, the modification of $\delta^{18}O$ in wood during the carbonization process was investigated in conjunction with elemental analysis, infrared spectroscopy (FTIR), and Rock-Eval thermal analysis, to explore the connection between the chemical composition of the materials and the alterations in $\delta^{18}O$. *Quercus petraea* wood samples were experimentally burned at temperatures ranging from 200°C to 1000°C under inert (pyrolysis) and oxidative atmospheres. The results reveal that the modification of $\delta^{18}O$ values

in charred wood can be described as a sequential two-step process. The initial step, occurring below 300°C, involves the volatilization and preferential degradation of thermolabile compounds, leading to an increase of +1.6 ‰ in $\delta^{18}O$. The subsequent step, below 700°C, results in a decrease in $\delta^{18}O$ values of -21.6 ‰, primarily driven by the thermal degradation of cellulose and lignin, as well as the increase of aromaticity and reorganization. The components and the $\delta^{18}O$ of wood undergo distinct changes in combustion mode, due to different carbonization kinetics as evidenced by FTIR and elemental analysis. To assess the intensity of the carbonization process, influenced by temperature, oxygen availability, and wood characteristics, the H/C atomic ratio, a good indicator of aromaticity, is used. A non-linear regression model was established, relating $\delta^{18}O$ to the H/C atomic ratio, thereby demonstrating that $\delta^{18}O$ values undergo changes as wood aromatization progresses, independent of the carbonization conditions. The second order model has a mean confidence interval of 1.9 ‰ and a prediction interval of 8.1 ‰. This work provides a fundamental understanding of the connection between the chemical composition of woody materials, alterations in $\delta^{18}O$, and the carbonization process, offering valuable insights for further studies and applications related to oxygen-related information that may be preserved in charcoals.

Keywords: oak; charcoal; $\delta^{18}O$; pyrolysis; combustion; FTIR

1. Introduction

Stable isotopes of carbon ($\delta^{13}C$) and oxygen ($\delta^{18}O$) in tree rings have proven useful for reconstructing past climate and water cycle variability, as well as better understanding tree ecophysiology (e.g. in temperate areas: [1–5]). These properties derive from the fact that environmental parameters (temperature, precipitation, solar radiation, air humidity) control the biological functions of trees, which, in turn, regulate $\delta^{13}C$ and $\delta^{18}O$ variations [6,7]. The

variability of $\delta^{13}C$ is mainly related to the stomatal regulation of gas fluxes into the leaf and the photosynthetic activity [8,9]. The $\delta^{18}O$ of plant tissues reflects the variation of $\delta^{18}O$ in precipitation and the subsequent evaporative fractionations that mainly take place in the soil and at the leaf level [10–13]. Thus, $\delta^{13}C$ and $\delta^{18}O$ in wood provide complementary climatic information.

The $\delta^{13}C$ of carbonized wood, especially archaeological charcoals, which are better preserved than wood in sediments over time, has been used to investigate paleoclimate [14–18]. Charcoals result from the incomplete combustion of woody material under an O_2-free or -restricted atmosphere [19,20]. Wildfires as well as anthropogenic fires cause heterogeneous charring of woody material with fast-burning high-temperature areas on the wood surface and smouldering lower-temperature regions in the interior [21,22].

Carbonization results in the modification of the physicochemical structure of wood. This change occurs through the progressive thermal degradation of wood constituents inducing the formation of stable aromatic rings and the reorganization of their structure into highly stable condensed compounds [21,23–29]. Consequently, in comparison to uncarbonized wood, charcoals are relatively enriched in carbon and aromatic moieties but are also depleted in hydrogen and oxygen as a consequence of the loss of functional groups [22,30,31].

The variation of $\delta^{13}C$ of wood under charring is generally between + 0.5 ‰ and – 2 ‰ (see review by [26]). Carbonization induces the preferential degradation of ^{13}C-enriched wood compounds (i.e., proteins, amino acids, holocellulose), resulting in a decrease of $\delta^{13}C$ close to the signature of the ^{13}C-depleted lignin [32,33]. The changes in $\delta^{13}C$ have been attributed mainly to kinetic effects related to temperature and the physiochemistry of the main wood components [34–36]. However, in contrast to the evolution of $\delta^{13}C$ during charring, the

behaviour of $\delta^{18}O$ remains poorly documented. Hatton et al. [37] reported ^{18}O enrichment in charred wood at temperature of less than 300°C (+ 0.5 ‰) and ^{18}O depletion at 600°C (- 15.9 ‰). Hamilton (master thesis) [38] also found an increase in $\delta^{18}O$ followed by a large decrease with increasing temperature in ambient and reduced atmosphere (+ 2.1 ‰ at 300°C and – 20 ‰ at 900°C during pyrolysis; + 1.8 ‰ at 300°C and -17.8 ‰ at 900°C during combustion). Nonetheless, the intensity of oxygen isotopic changes in relation to the chemical modifications that occur during carbonisation needs to be better understood since each component is differently altered and modified as charring progresses.

Therefore, our study aims to document the progressive changes of wood $\delta^{18}O$ in relation to the transformation of organic matter during carbonization. We measured the $\delta^{18}O$ of oak wood experimentally burnt between 200°C and 1000°C in inert (nitrogen pulsed gas) and oxidative (air) atmospheres to characterize the changes of $\delta^{18}O$ in wood. Elemental analyses, infrared spectroscopy and Rock-Eval® thermal analyses were conducted to investigate potential links between the evolution of the chemical components of the studied materials and $\delta^{18}O$ modifications.

2. Material and methods

2.1. Experimental design

Approximately 200 mg of crushed oak (*Quercus petraea*; Ø ~ 50 µm) was heated in quartz tubes plugged with SiO_2 wool. The samples were placed for one hour in a preheated tubular furnace set at 200, 250, 300, 350, 400, 450, 500, 600, 700, 800, 900, and 1000°C. They were held under a constant flow of N_2 (≥ 99,8 %) to produce charcoal via pyrolysis. After heating, the samples were cooled to room temperature (ca. 20°C) outside of the oven. A similar experiment with different aliquots was conducted for the Rock-Eval® thermal analysis.

Experimental carbonization was also conducted under an ambient atmosphere (in the presence of O_2) as an approach to produce charcoal through combustion. The powders were heated for one hour in ceramic crucibles in air using a preheated muffle furnace set at 200, 250, 300, 350, 400, 450, and 500°C. It is worth mentioning that above 350°C, only ash remained after one hour of thermal treatment.

Each experiment was replicated three times. All samples were weighed before and after heating to determine mass loss (data are available in Supplementary Material; Fig. S2).

2.2. Elemental and Rock-Eval® thermal analyses

Carbon (C), hydrogen (H), and oxygen (O) contents (wt%) were measured with a Thermo-Fisher Flash 2000 analyser. Ca. 2 mg of samples were weighed in tin capsules for C and H and in silver capsules for O. International standards were used to calibrate the values. The uncertainties were ± 0.5 % for C, ± 0.7 % for H and ± 3 % for O. Carbon and hydrogen were determined simultaneously following combustion, while oxygen was determined following a pyrolysis process. The elemental composition of the ash obtained after burning samples above 300°C was not measured.

Rock-Eval® thermal analysis was conducted using less than 10 mg of materials with a Rock-Eval® 6 turbo device designed by Vinci Technologies. The basic operating principles of this method have been presented by Behar et al. [39]. Briefly, Rock-Eval® thermal analyses consist of two stages: pyrolysis, followed by combustion. In the following section, we focus on the pyrolysis stage. Programmed pyrolysis (under N_2) takes place in two phases: (i) a three-minute-long isothermal phase at 300°C (corresponding to the "S1 peak"), followed by (ii) a pyrolysis phase performed at an increasing temperature from 300 to 800 °C at a rate of 25 °C/min. During these two phases, hydrocarbons (HC), on the one hand, and CO and CO_2, on the other hand, are continuously quantified with flame ionization and infrared detectors, respectively.

Quantification of HC released during the first isothermal phase provides the S1 peak parameter related to free and thermodesorbable HC [39].

2.3. Fourier transform mid-infrared spectroscopy (FTIR)

The samples were dried overnight (50°C) to eliminate moisture before being analyzed. FTIR analyses were performed using a Bruker Tensor 27 spectrometer equipped with a germanium crystal in attenuated total reflectance (ATR) mode. FTIR spectra were acquired over the 4000–600 cm^{-1} spectral range, with a spectral resolution of 4 cm^{-1} and 64 scans. Spectra were corrected for atmospheric interference (H_2O and CO_2) and differences in beam penetration depth at different wavelengths (ATR correction) using Opus software. FTIR absorption bands were assigned on the basis of literature (Table 1).

2.4. Isotopic analysis

The $\delta^{18}O$ was determined using a high-temperature conversion elemental analyzer (TC- EA, Thermo Scientific) coupled with an Isotope Ratio Mass Spectrometer (IRMS, IsoPrime). 0.2 to 1 mg of charcoal material was weighed in silver capsules (data are available in Supplementary Material; Fig. S1), converted to CO by pyrolysis at 1400°C, and then flushed into a mass spectrometer. The isotope ratio values are expressed in Eq. 1 according to the δ notation:

$$\delta\ (‰) = [(^{18}O/^{16}O_{sample})/(^{18}O/^{16}O_{standard}) -1] \times 1000 \quad (1)$$

Where $^{18}O/^{16}O_{standard}$ refers to the oxygen isotopic ratio of the Vienna Standard Mean Ocean Water (V-SMOW)

). Along the sequence of analyses, the isotopic composition of CC31, an internal laboratory reference for cellulose, was measured every three samples. The $\delta^{18}O$ of CC31 (set by consensus between 9 European laboratories; [40]) is 31.85 ‰. A one-point calibration was applied using

this reference value. The long-term analytical precision based on repeated measurements of CC31 cellulose was within 0.20 ‰.

The effect of charring on wood isotope composition is further expressed as Eq. 2:

$$\Delta^{18}O_{char}\ (‰) = \delta^{18}O_{char} - \delta^{18}O_{initial} \quad (2)$$

where $\delta^{18}O_{initial}$ represents the $\delta^{18}O$ value of uncharred oak ($\delta^{18}O_{initial}$ = 24.66 ‰), and $\delta^{18}O_{char}$ is the mean value of charred materials formed at a given temperature (between 200 and 1000°C).

2.5. Statistics

Pearson correlation coefficients and second order polynomial regression as well as confidence and prediction intervals were calculated using XLSTAT 2023 1.1 (https://www.xlstat.com/fr).

3. Results

3.1. Elemental and Rock-Eval® thermal analyses

The oxygen (O) and hydrogen (H) contents decreased substantially with increasing pyrolysis temperature from 42.00 % and 5.82 % to 3.71 % ± 1.00 and 0.49 % ± 0.11, respectively, at 1000°C (Table S1 & S2). At 400°C, with 25.53 % ± 2.33 wood had almost lost half of its initial oxygen content. The C content continuously increased from 47.09 % to 83.91 % ± 5.09 at 1000°C. The atomic ratios decreased with temperature, as illustrated in the H/C versus O/C diagram (so-called van Krevelen diagram; [41]; Fig. 1). Pyrolysis charcoals exhibit a H/C ratio decreasing continuously from 1.47 ± 0.04 at 200°C to 0.07 ± 0.01 at 1000°C. The O/C ratio decreased from 0.68 ± 0.01 to 0.03 ± 0.01 in the same temperature range.

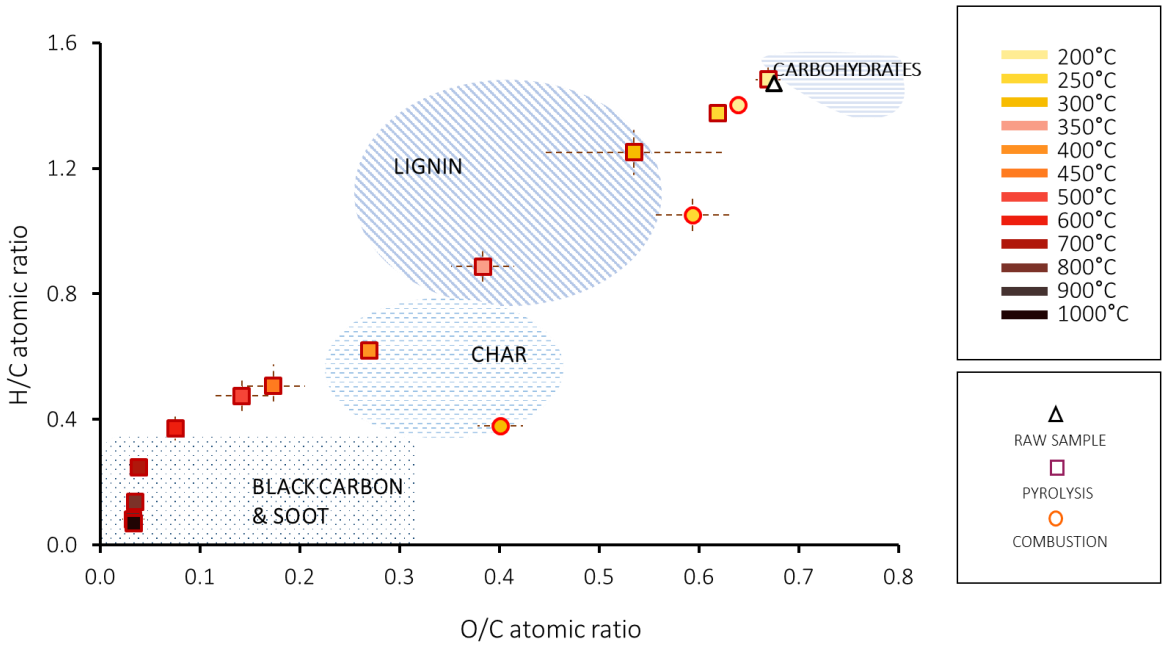

Fig. 1. H/C and O/C atomic ratios determined in wood carbonized from 200°C to 1000°C in pyrolysis and combustion (n=3; the standard deviation is indicated in dotted lines). The carbohydrates, lignin-derived, char-, black carbon- soot fields are inspired from Hammes et al. [42].

The H and O contents of the charred wood is much lower when carbonization was obtained under combustion compared to pyrolysis at a given temperature. For example, at 300°C, the H content was 5.49 ± 0.10 % during pyrolysis, while it decreased to 1.92 ± 0.14 % during combustion. At the same temperature, the O content was 38.23 ± 1.37 % during pyrolysis, while it reached 32.50 ± 0.71 % during combustion. The H/C and O/C ratios decreased continuously during combustion (Fig. 1). The wood was completely consumed at 350°C in combustion, leaving only ash.

The Rock-Eval® thermal analyses revealed that a significant quantity of volatile products was released (CO, CO_2, and HC) during the pyrolysis experiments, in particular between 200°C and

400°C (Fig. 2). More specifically, the S1 peak decreased from 54.4 mg/g at 200°C to 1.4 mg/g at 400°C, and less than 1.2 mg/g at 1000°C (Fig. 2 and Table S3). Beyond 400°C in pyrolysis, we observe that CO, CO_2, and HC emissions were asynchronous (Fig. S3).

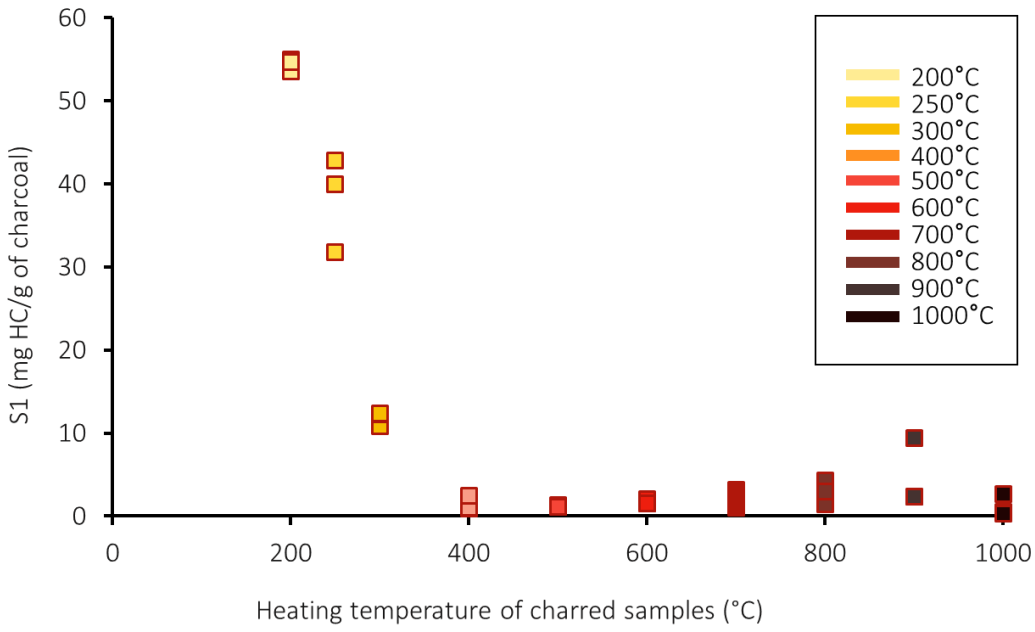

Fig. 2. S1 peak (300°C isothermal phase) measured by Rock-Eval® on charred wood heated in pyrolysis from 200°C to 1000°C.

3.2. Fourier-transform infrared spectroscopy

The infrared spectra of the raw sample showed absorption bands assigned to C-H, C-O, OH, and aromatic skeletal vibration functions (Fig. 3 and Table 1). The intensity of absorption bands (1) in the 3600-3000 cm^{-1} range and (2) at 1040 cm^{-1}, assigned to (1) OH stretching and (2) aliphatic and alcohol C-O stretching vibrations, respectively, [43] were substantially reduced between 300 and 400 °C. (Fig. 3a and Table 1). The C-H aliphatic stretching vibration group (2930 cm^{-1}) showed a similar trend, that is, a rapidly decreasing intensity with increasing temperature, becoming almost undetectable above 400 °C.

Below 700°C, the intensity of the band observed between 1704 cm^{-1} and 1735 cm^{-1} (C=O stretching; [44]) decreased. Between 400 and 700°C, the relative intensity rise in the C=C aromatic skeletal vibration and the presence of a C=O stretching band (1596-1606 cm^{-1}) attested to the progressive aromatization of organic matter with increasing carbonization temperature [45] (Fig. 3a and Table 1). In addition, absorption bands assigned to skeletal C-C vibration and C-O and O-H bending (1150, 1235, 1370, 1420, and 1460 cm^{-1}) merged in a broad band occurring between 1150 and 1460 cm^{-1} [46]. From 800°C onwards, IR spectra showed a general decrease in intensity until the bands were no longer visible.

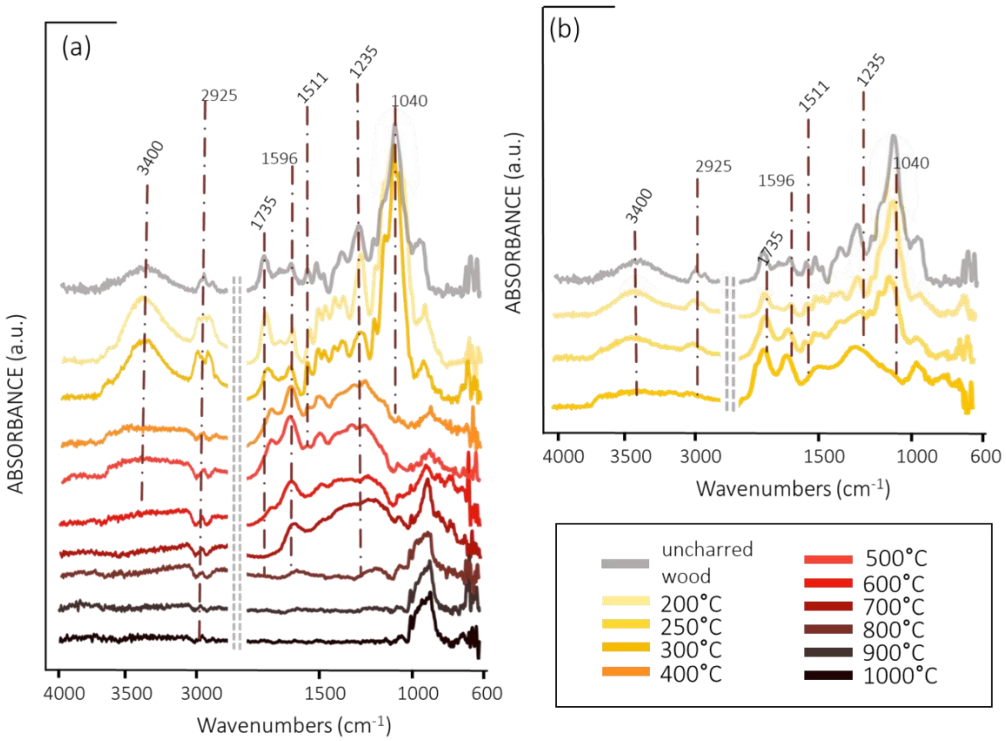

Fig. 3. FTIR-ATR spectra of oak samples charred **(a)** between 200°C and 1000°C in pyrolysis and **(b)** between 200°C to 300°C in combustion. The brown dotted lines indicate the characteristic wood peaks reported in the literature and described in Table 1.

Table 1. Major IR absorption bands and assignments.

Wavenumber (cm^{-1})	**Peak assignment**
3400	-O-H stretching[43,44,46]
2925	Aromatic and aliphatic C-H and CH_2 stretching in methyl and methylene[43,44,46]
1735-1704	Non-conjugated C=O in hemicellulose and aromatic carbonyl[43,44,47]
1596	Aromatic skeletal vibration in lignin[48,49]
1505-1512	Aromatic skeletal vibration in lignin [43,44,46,48,49]
1460	C-H deformation in lignin and carbohydrates[44,49]
1423	Benzene skeletal combined with C-H deformation[44,48]
1370	Aliphatic C-H stretching in methyl and phenol O-H[47]
1325	C-H vibration in cellulose and C-O vibration in lignin units[48,49]
1235	C-O stretching in lignin units and bending O-H, antisymmetric stretching vibration of the acetyl ester groups[44,47–49]
1150	C-O-C stretching[47–49]
1040	Aliphatic ether C–O and alcohol C–O stretching in cellulose and hemicellulose[43,46,49]
895	aromatic C-H out of plane deformation[46,47]
Guo & Bustin, 2018 [43] ; Esteves et al. 2013 [44]; Yu et al. 2018 [46]; Lehto et al. 2018 [47]; Gonultas et al. 2018 [48] ; Kwon et al. 2013 [49]	

The band between 800 and 950 cm^{-1}, persisting to 1000°C, will not be discussed here as an assignment to Si-O vibration (due to remnants of glass fibers from the experimental device) cannot be ruled out unambiguously.

The structural modifications undergone by the wood during pyrolysis were different from those undergone during combustion at the same temperature. It could have been similarities between spectra obtained from different temperature such as the resemblance between spectra at 300°C from combustion and those from 400°C in pyrolysis which experienced the disappearance of the cellulosic band (1040 cm^{-1}). However, it should be noted that the FTIR spectra exhibit a distinct disparity in the band ratio of 1735/1600 cm^{-1} related to the carbonization process (Figs. 3b, Table. S1; 1730/1600).

3.3. Oxygen isotopic composition

$\delta^{18}O$ values are presented in Table S1 and averaged in Supplementary Material (Table S2).

During the pyrolysis experiments at temperatures lower than 300°C, the $\Delta^{18}O_{char}$ values no longer equals zero and increases slightly, indicating an ^{18}O-enrichment of the heated wood compared to the raw wood (maximum values of $\Delta^{18}O_{char}$ at 300°C: + 1.6 ± 0.2 ‰). Such slight increases were also observed in charred wood produced by combustion, but at 200°C ($\Delta^{18}O_{char}$ = + 0.7 ± 0.2 ‰ at 200°C) (Fig. 4 and Table S2).

This enrichment was followed by an overall decrease in $\Delta^{18}O_{char}$ from -1.9 ± 0.5 ‰ at 350°C to -24.6 ± 3.6 ‰ at 1000°C. The largest isotopic shift observed between fresh and charred wood was -29.6 ‰ (± 1σ = 0.5, n=3), at 900°C during pyrolysis. $\Delta^{18}O_{char}$ was highly correlated with pyrolysis temperature (r = - 0.95; p-value < 0.05).

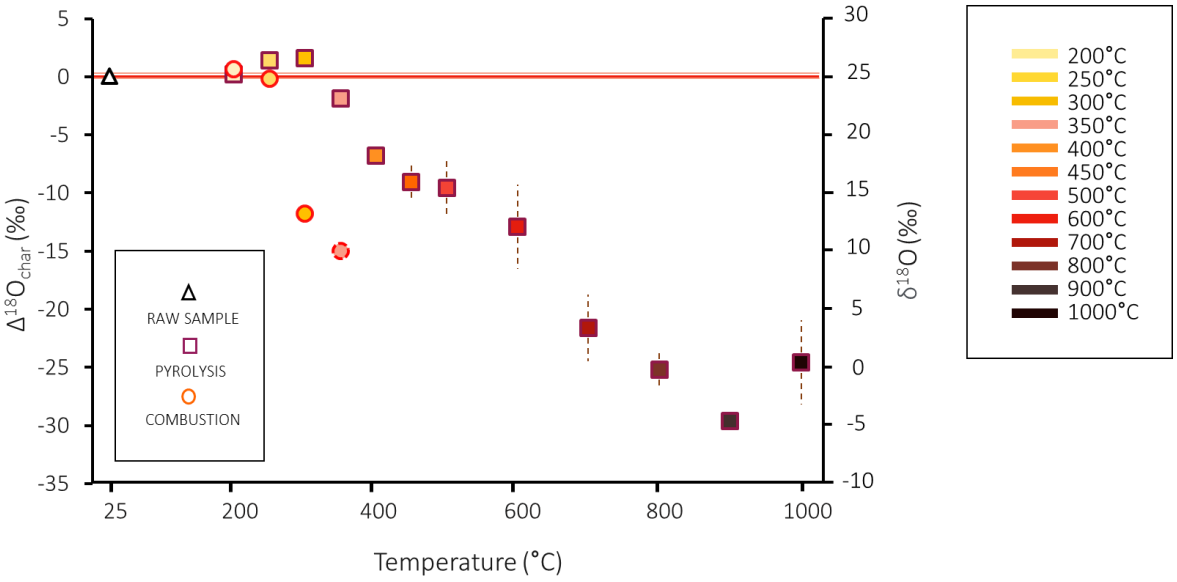

Fig. 4. Mean $\Delta^{18}O_{char}$ measured in wood carbonized from 200°C to 1000°C in pyrolysis and combustion (n=3 except for 350°C sample in combustion for which, n=1; the standard deviation is indicated as dotted lines). The bold red line represents the raw sample with 0.2 ‰ measurement uncertainty.

For a given temperature, $\Delta^{18}O_{char}$ values were notably different in the pyrolysis and combustion experiments. For instance, at 300°C, $\Delta^{18}O_{char}$ are respectively +1.6 ‰ ± 0.2 and -11.8 ‰ ± 0.8 (Fig. 4 and Table S2). Furthermore, two samples remaining after combustion above 300°C exhibited $\Delta^{18}O_{char}$ values -14.99 ‰ and -14.53 ‰ at 350°C and 500°C, respectively (Table S1).

During pyrolysis, the standard deviation of oxygen isotopic ratio among the replicates remained lower than the mass spectrometer uncertainty (± 0.2 ‰) below 400°C. At higher temperatures, the difference between the $\Delta^{18}O_{char}$ values of the three experimental replicates was as high as ± 3.6 ‰ (mean for 1000°C).

4. Discussion

4.1. How and why does $\delta^{18}O$ change with increasing temperature during pyrolysis?

The increase in pyrolysis temperature mainly results in two distinct $\Delta^{18}O_{char}$ modifications: (1) a slight increase (ca. + 1.5 ‰) between 200 and 300°C and (2) a broad decrease (ca. -21.5 ‰; Fig. 4 and Table S1) up to 700 °C. Beyond 800°C, no clear effect of carbonization was evidenced either on the chemical structure or on the $\delta^{18}O$ values of the charred wood.

Between 200 and 300°C, the $\Delta^{18}O_{char}$ increase is related with the decrease in H/C and O/C due to the loss of unbound and structural waters as well as the thermal desorption/degradation of hydrocarbons (Figs. 1 and 2, Table S1; [23,36,37]). In addition, the decrease of intensity in

carbonyl groups bands observed in FTIR spectra at 1735 cm^{-1} (Fig. 3 and Table 1) is consistent with the thermal decomposition of hemicellulose initiated between 200°C and 300°C as described by Cheng et al. [50] and Yang et al. [30]. However, in these two studies, the investigations were conducted on pure hemicellulose, the thermal decomposition of which may have a different behaviour when it is interconnected with other components in wood [51]. Furthermore, the $\delta^{18}O$ of the hemicellulose is similar or slightly higher than that of the whole wood [52]. Thus, the thermal degradation of this component cannot account for the observed increase in $\Delta^{18}O_{char}$. Hence, the initial increase in $\Delta^{18}O_{char}$ may rather reflect the loss of residual water, depleted in ^{18}O compared to the wood [12,13], and possibly the decomposition of unidentified ^{18}O-depleted organic component. Czimczik et al. [23] interpreted a ^{13}C enrichment of charred wood at 150°C by the loss of ^{13}C depleted lipids. A similar process may take place here for the $\delta^{18}O$ increase as lipids are also ^{18}O depleted with respect to bulk wood [53].

The second phase in the thermal decomposition is marked by a notable decline of $\Delta^{18}O_{char}$ from 350°C to 700°C. This phase consists in (i) the thermal degradation of the main constituents of wood (e.g. hemicellulose, cellulose, and lignin; Fig. 4; [54,55]) and (ii) the increase in the degree of aromaticity of the carbonized wood (Fig. 1, Table S1; [24]).

Below 400°C, the thermal degradation of carbohydrates, including cellulose, takes place through depolymerization, as illustrated by the disappearance of their characteristic FTIR bands at 1040 and 1735 cm^{-1} (Fig. 3 and Table 1; [43,56]). As cellulose is ^{18}O-enriched compared to bulk wood material [26,57–59], its thermal degradation could lead to the decline of $\Delta^{18}O_{char}$. However, in our experiments the depletion in ^{18}O is accentuated above 400°C, while the thermal degradation of cellulose has almost been completed by that temperature (Fig. 4; [20,30]). Therefore, the decreasing trend of $\Delta^{18}O_{char}$ with temperature suggests that the thermal degradation of cellulose can only partially explain the evolution of $\Delta^{18}O_{char}$ with temperature.

Between 400 and 700°C, the FTIR spectra indicate the progressive decrease in the intensity of carbonyl, carboxyl, methoxy and phenolic hydroxyl groups bands with temperature (Figs. 1 and 3; Tables 1 and S1), which can be assigned to lignin depolymerization [54,60,61]. Aromatization also takes place during the wood thermal degradation as shown by the progressive increase of the C=C aromatic vibration in the FTIR spectra (Fig. 3 and Table 1). This conclusion was also drawn by Hatton et al. [37], Li et al. [55], McBeath et al. [24] and Mouraux et al. [35]. Lignin exhibits a lower $\delta^{18}O$ value compared to the whole wood (between 10.2 and 15.4 ‰; [32,38]). Nevertheless, the relatively low $\delta^{18}O$ value of lignin may not be sufficient to explain a low $\delta^{18}O$ of 3.0 ± 2.9 ‰ as observed in charcoals at 700°C. For instance, the $\delta^{18}O$ of oxygenated functional groups in vanillin which can be derived from the thermal transformation of lignin, show large variations between carbonyl, methoxy and phenolic hydroxyl groups [62]. Indeed, in comparison to carbonyl oxygen, with a $\delta^{18}O$ of ca. 26.2 ‰, methoxy and phenolic hydroxyl groups exhibited $\delta^{18}O$ as low as 2.7 and 5.8 ‰, respectively. The decline in $\Delta^{18}O_{char}$ from 400 to 700°C may then be attributed to the selective and relative preservation of the ^{18}O-depleted methoxy and phenolic hydroxyl groups (Fig. 3 and Table 1). The evidence that these groups exist at these temperature [37,54,56,63,64] supports this hypothesis.

Above 800°C, the evolution of O/C atomic ratio as well as FTIR spectra do not reveal any changes in the chemical structure of the charcoals because of the limits of the precision and the resolution of the analytical approach and the inability of FTIR to detect carbon covalent bonds (Fig. 3, Table S1 and S2). Between 800 and 1000°C, the uncertainties on $\Delta^{18}O_{char}$ are ± 1.5 ‰ and ± 3.6 ‰, respectively. Such variability in $\Delta^{18}O_{char}$ may reflect differences in the proportions of the various compounds between the replicates. However, increased pyrolysis temperatures imply an overall degradation of oxygenated functional groups, which should theoretically smooth out intrinsic heterogeneity related to organics. We hypothesize that the observed

variability of $\Delta^{18}O$ at a given temperature can be ascribed to changes in the concentration of inorganic sources of O in the charred wood or to small changes in the experimental conditions between replicates.

4.2. Why is the reproducibility of the $\delta^{18}O$ measurements low above 400°C?

Wood contains a variety of mineral elements with calcium, potassium and magnesium being the most abundant cations [65,66]. The concentrations in mineral elements are neither constant across growth rings [66], nor along the stem (e.g. [67]). These elements exist as oxides, oxalates, carbonates, phosphates and sulphates in the wood [64,68]. Minerals usually correspond to < 1 wt% of wood and the mineral content of charred wood increases with increasing charring temperature [69]. In oaks, Ca-oxalate (CaC_2O_4) and silica (SiO_2) are the most common minerals [68,70].

It has been shown that the interactions between wood constituents and mineral elements naturally present in the biomass, can modify thermochemical processes and promote the rearrangement of aromatic rings above 350°C [54]. They could also alter the yields of lignocellulose-derived compounds [71,72].

In this study, CO, CO_2, and HC emissions are asynchronous above 400°C during the Rock-Eval® thermal experiment (Fig. S3). This suggests a contribution from an inorganic component, such as calcite, to CO and CO_2 emissions at these temperatures. Actually, calcite has already been detected by X-ray diffractometry in *Fagus* and *Picea* samples pyrolyzed at 600°C and in biochar of hardwood and softwood heated at 450°C [31,73]. Its formation was suggested to follow the transformation of Ca-oxalate present in uncharred wood. The formation of quartz and cristobalite during wood carbonisation has also been described [73].

As the oxygen from organic molecules is progressively lost above 400°C, the contribution of oxygen from minerals to the overall $\delta^{18}O$ of the charred wood may increase with increasing temperature [63,74,75]. However, since the nature and the distribution of the minerals in the original wood were not determined, we cannot evaluate their contribution to $\delta^{18}O$.

4.3. Does the oxygen supply during the carbonization process impact the oxygen isotope ratio?

Within a fire, conditions change from the heart to the periphery of the blaze. The oxygen availability, being uniform neither in space nor time, depends on the fire regime and severity [29,76–78]. Therefore, documenting the modification of $\delta^{18}O$ under both pyrolysis and oxidizing conditions is a required first step to enable interpretation of the oxygen isotopic composition of charcoals.

At a given temperature, the depletion in H and O contents and the decrease in $\Delta^{18}O_{char}$ are larger in combustion than in pyrolysis mode (Figs. 1 and 4, Table S1). The presence of oxygen during wood charring impacts various physicochemical properties, such as the mass loss, the aromatic C content, and the isotopic composition of the residual char [34,79–81]. The pyrolysis and combustion processes involve different chemical and physical reactions [81–84], which necessarily lead to differences in kinetic or equilibrium isotopic effects.

For a given value of $\delta^{18}O$, the structural composition of the charcoal is not the same in pyrolysis and combustion experiments, as shown by the infrared spectroscopy results. For example, the $\Delta^{18}O_{char}$ of -12.9 ± 3.6 ‰ in the wood pyrolyzed at 600°C, is close to the value of – 11.76 ± 0.8 ‰ in the wood sujected to combustion at 300°C, but the 1735 cm^{-1} band is much shorter in the former than in the latter (Fig. 3, Table S2). Moreover, Li et al. [85] showed that the relative absorbance of this band, attributed to the carbonyl (C=O) bond, increased with temperature

during carbonization under oxidative conditions, which is not the case under pyrolysis conditions. This reaction could be due to the fragmentation of aliphatic side chains in lignin or the cleavage of β-O-4 linkages [85]. Nevertheless, the different structural changes between pyrolysis and combustion do not significantly affect the charcoal's isotopic composition. Indeed, $\Delta^{18}O_{char}$ parameters follow similar changes along the two experiments, albeit at different rates. Consequently, these isotopic alterations appear to be primarily driven by the degradation of the main components, although we cannot entirely rule out the possibility of minor isotope exchanges with atmosphere in combustion experiments.

4.4. Can the original $\delta^{18}O$ value of wood be inferred from its burnt counterpart?

More than temperature, the intensity of the carbonization) induces the degradation and structural changes in the wood components that drive the modification of $\delta^{18}O$. The intensity of carbonization depends both on temperature and oxygen availability since at a given temperature, the carbonization and pyrolysis do not produce the same results. In addition, other characteristics of the wood such as its moisture content, chemical composition (including its mineral content), density, and porosity as well as the size and shape of the wood particles may affect the evolution of the isotopic composition under heat treatment [23,26,34,36].

Given the observed differences in the physicochemical and oxygen isotopic composition of the charred wood between the two fire regimes, the O/C atomic ratio hardly provides an independent assessment of the intensity of carbonization (Fig. S4). On the contrary, the H/C atomic ratio decreases with the growth and subsequent progressive condensation of aromatic rings, which take place with the intensification of the charring process [27,86]. We thus propose

to use the H/C atomic ratio as a proxy for the intensity of carbonization. $\Delta^{18}O_{char}$ decreases with decreasing H/C, both in pyrolysis and combustion experiments (Fig. 5). A non-linear 2nd order regression model can be fitted to the data as Eq. 3:

$\Delta^{18}O_{char} = -31.2 + 54.3 \times (H/C) - 22.5 \times (H/C)^2$ with a 95 % mean confidence interval of 1.9 ‰ and a prediction interval of 8.1 ‰ (3)

This regression can theoretically be used to estimate the original oxygen isotopic composition of wood samples burned by combustion or pyrolysis from their H/C and $\delta^{18}O$ (Fig. 5). However, this approach can only provide a rough indication of the pristine $\delta^{18}O$ because the variation of the wood $\delta^{18}O$ during carbonization is very large compared to the natural variability in time and space of wood $\delta^{18}O$ (typically a few per mil, e.g in oaks : [87–90]). In addition, the model uncertainty is large, which precludes a precise determination of $\Delta^{18}O_{char}$. Moreover, the model defined in this study may not be transposable to the wood of another tree species, or even to the wood of another oak. Indeed, the evolution of $\Delta^{18}O_{char}$ as a function of carbonization intensity may change from one wood to another because the proportions of the main components and their molecular stability, which control the isotopic signature, are variable. Furthermore, even if the H/C is known to be a good index of the aromaticity of organic matter [27,86], the proportions of lignin, cellulose and hemicelluloses, which vary from one species to another, affect the H/C. Therefore, comparative studies on different species would be necessary to strengthen the model.

In addition, it has to be acknowledged that experimental charcoals are not subjected to the same post-depositional and diagenetic conditions as charcoals found in the natural environment. Indeed, oxidation and sorption can alter the O/C and H/C ratios during the diagenesis process [91,92]. Hence, the application of the model to H/C ratios affected by diagenesis may lead to misinterpretations. Moreover, it is worth noting that no research has investigated the potential

influence of oxidation and sorption on the $\delta^{18}O$ isotopic signature of charcoal during post-depositional processes. Consequently, it is imperative to ascertain, prior to referencing the model, that the chemical composition of the charcoal has not undergone substantial alteration.

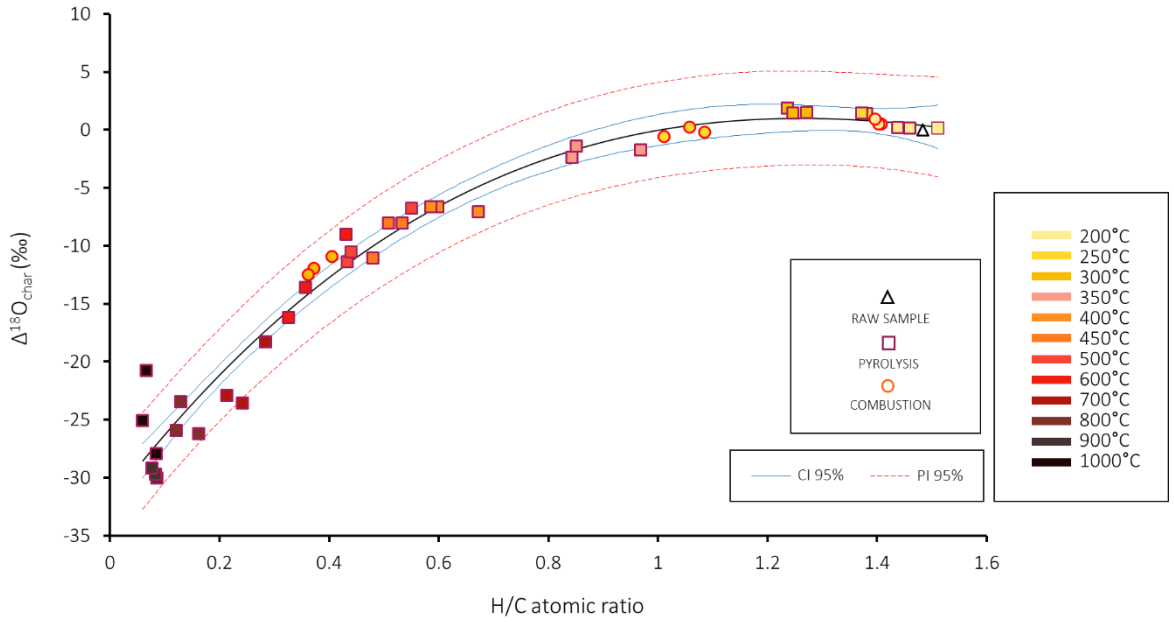

Fig. 5. Nonlinear regression (black line) modelling the relationship between $\Delta^{18}O_{char}$ ratios and H/C atomic ratios from wood samples charred between 200°C and 1000°C in pyrolysis and combustion. The blue lines represent 95 % confidence interval while red dotted lines represent 95 % prediction intervals.

5. Conclusion

Carbonization induces significant physical, elemental, and structural transformations in *Quercus petraea* wood. The modification of $\delta^{18}O$ values in pyrolysis wood products can be characterized as a two-step process. The initial step (<300°C) is influenced by the volatilization and preferential degradation of labile compounds, as well as the loss of free and non-structural water. During this step, $\delta^{18}O$ increases. The subsequent step (<700°C) is primarily driven by

the thermal degradation of wood cellulose and lignin. During this step, $\delta^{18}O$ drastically decreases.

Combustion induces different changes to pyrolysis, in particular different oxygen bond rearrangement in the material as shown by FTIR and elemental analysis. The overall evolution of $\delta^{18}O$ during combustion differs from pyrolysis. Indeed, the intensity of the carbonization process, not only influenced by temperature but also oxygen availability, and various wood characteristics, primarily drives the modification of $\delta^{18}O$. The H/C ratio, which reveals the degree of aromatization of the organic material, reflects the progress of carbonization, whether by combustion or pyrolysis. $\Delta^{18}O_{char}$ changes systematically as a function of H/C according to a non-linear model. The application of the model to $\Delta^{18}O_{char}$ - H/C data from charcoal does not allow to track back to an initial $\delta^{18}O$ value in the wood with confidence, in particular because of large model uncertainties. However, for an H/C >1, the $\Delta^{18}O_{char}$ measured do not undergo large changes compared to their initial value (<2 ‰) which should encourage the development of this function especially on charcoal heated at low carbonization intensity.

Ideally, each fraction should be identified, such as the $\delta^{18}O$ linked to the physiological process involved in its formation. However, our approach is limited to an empirical quantification of the oxygen isotope fractionation process at different structural stages of carbonization product formation in *Quercus petraea*. Ideally, to refine the model and provide the theoretical fundamentals of $\delta^{18}O$ changes with H/C, each molecular compound in the wood should be identified, and its $\delta^{18}O$ determined.

Acknowledgements

This research was supported by the "ANR-Agence Nationale de la Recherche" (CASIMODO project; ANR-20-CE03-0008). We owe great thanks to Monique Pierre and Michel Stievenard

(UMR 1572 LSCE, CEA/CNRS) for isotope measurements. We are also grateful to Christelle Anquetil for her help with the FTIR-ATR facilities (UMR 7619 METIS, CNRS).

Author contributions

D.dB.: Formal analysis; Investigation; Visualization; Writing - original draft, review & editing. **F.D.**: Conceptualization; Investigation; Formal analysis; Resources; Supervision; Validation; Writing - original draft, review & editing. **V.D**.: Formal analysis; Resources; Supervision; Validation; Writing - original draft, review & editing. **T.T.N.T**.: Resources; Supervision; Validation; Writing - original draft, review & editing **F.B.**: Investigation; Writing- review & editing. **A.D.**: Funding acquisition; Project administration; Supervision; Writing - original draft, review & editing.

References

[1] M. Saurer, U. Siegenthaler, F. Schweingruber, The climate-carbon isotope relationship in tree rings and the significance of site conditions, Tellus B. 47 (1995) 320–330. https://doi.org/10.1034/j.1600-0889.47.issue3.4.x.

[2] S. Ponton, J.-L. Dupouey, N. Bréda, F. Feuillat, C. Bodénès, E. Dreyer, Carbon isotope discrimination and wood anatomy variations in mixed stands of Quercus robur and Quercus petraea, Plant Cell Environ. 24 (2001) 861–868. https://doi.org/10.1046/j.0016-8025.2001.00733.x.

[3] N. Etien, V. Daux, V. Masson-Delmotte, O. Mestre, M. Stievenard, M.T. Guillemin, T. Boettger, N. Breda, M. Haupt, P.P. Perraud, Summer maximum temperature in northern France over the past century: instrumental data versus multiple proxies (tree-ring isotopes, grape harvest dates and forest fires), Clim. Change. 94 (2009) 429–456. https://doi.org/10.1007/s10584-008-9516-8.

[4] I. Labuhn, V. Daux, M. Pierre, M. Stievenard, O. Girardclos, A. Féron, D. Genty, V. Masson-Delmotte, O. Mestre, Tree age, site and climate controls on tree ring cellulose δ18O: A case study on oak trees from south-western France, Dendrochronologia. 32 (2014) 78–89. https://doi.org/10.1016/j.dendro.2013.11.001.

[5] K. Treydte, S. Boda, E. Graf Pannatier, P. Fonti, D. Frank, B. Ullrich, M. Saurer, R. Siegwolf, G. Battipaglia, W. Werner, A. Gessler, Seasonal transfer of oxygen isotopes from precipitation and soil to the tree ring: source water versus needle water enrichment, New Phytol. 202 (2014) 772–783. https://doi.org/10.1111/nph.12741.

[6] D. McCarroll, N.J. Loader, Stable isotopes in tree rings, Quat. Sci. Rev. 23 (2004) 771–801. https://doi.org/10.1016/j.quascirev.2003.06.017.

[7] M. Gagen, G. Battipaglia, V. Daux, J. Duffy, I. Dorado-Liñán, L.A. Hayles, E. Martínez-Sancho, D. McCarroll, T.A. Shestakova, K. Treydte, Climate Signals in Stable Isotope Tree-Ring Records, in: R.T.W. Siegwolf, J.R. Brooks, J. Roden, M. Saurer (Eds.), Stable

Isot. Tree Rings Inferring Physiol. Clim. Environ. Responses, Springer International Publishing, Cham, 2022: pp. 537–579. https://doi.org/10.1007/978-3-030-92698-4_19.
[8] G.D. Farquhar, J. Lloyd, 5 - Carbon and Oxygen Isotope Effects in the Exchange of Carbon Dioxide between Terrestrial Plants and the Atmosphere, in: J.R. Ehleringer, A.E. Hall, G.D. Farquhar (Eds.), Stable Isot. Plant Carbon-Water Relat., Academic Press, San Diego, 1993: pp. 47–70. https://doi.org/10.1016/B978-0-08-091801-3.50011-8.
[9] L.A. Cernusak, N. Ubierna, Carbon Isotope Effects in Relation to CO2 Assimilation by Tree Canopies, in: R.T.W. Siegwolf, J.R. Brooks, J. Roden, M. Saurer (Eds.), Stable Isot. Tree Rings Inferring Physiol. Clim. Environ. Responses, Springer International Publishing, Cham, 2022: pp. 291–310. https://doi.org/10.1007/978-3-030-92698-4_9.
[10] R.L. Burk, M. Stuiver, Oxygen isotope ratios in trees reflect mean annual temperature and humidity, Science. 211 (1981) 1417–1419. https://doi.org/10.1126/science.211.4489.1417.
[11] J.S. Roden, G. Lin, J.R. Ehleringer, A mechanistic model for interpretation of hydrogen and oxygen isotope ratios in tree-ring cellulose, Geochim. Cosmochim. Acta. 64 (2000) 21–35. https://doi.org/10.1016/S0016-7037(99)00195-7.
[12] M.M. Barbour, T.J. Andrews, G.D. Farquhar, Correlations between oxygen isotope ratios of wood constituents of Quercus and Pinus samples from around the world, Funct. Plant Biol. 28 (2001) 335–348. https://doi.org/10.1071/pp00083.
[13] X. Song, A. Lorrey, M.M. Barbour, Environmental, Physiological and Biochemical Processes Determining the Oxygen Isotope Ratio of Tree-Ring Cellulose, in: R.T.W. Siegwolf, J.R. Brooks, J. Roden, M. Saurer (Eds.), Stable Isot. Tree Rings Inferring Physiol. Clim. Environ. Responses, Springer International Publishing, Cham, 2022: pp. 311–329. https://doi.org/10.1007/978-3-030-92698-4_10.
[14] J.P. Ferrio, N. Alonso, J.B. López, J.L. Araus, J. Voltas, Carbon isotope composition of fossil charcoal reveals aridity changes in the NW Mediterranean Basin, Glob. Change Biol. 12 (2006) 1253–1266. https://doi.org/10.1111/j.1365-2486.2006.01170.x.
[15] G. Hall, S. Woodborne, M. Scholes, Stable carbon isotope ratios from archaeological charcoal as palaeoenvironmental indicators, Chem. Geol. 247 (2008) 384–400. https://doi.org/10.1016/j.chemgeo.2007.11.001.
[16] M. Aguilera, C. Espinar, J.P. Ferrio, G. Pérez, J. Voltas, A map of autumn precipitation for the third millennium BP in the Eastern Iberian Peninsula from charcoal carbon isotopes, J. Geochem. Explor. 102 (2009) 157–165. https://doi.org/10.1016/j.gexplo.2008.11.019.
[17] F. Baton, T.T. Nguyen Tu, S. Derenne, A. Delorme, F. Delarue, A. Dufraisse, Tree-ring δ13C of archeological charcoals as indicator of past climatic seasonality. A case study from the Neolithic settlements of Lake Chalain (Jura, France), Quat. Int. 457 (2017) 50–59. https://doi.org/10.1016/j.quaint.2017.03.015.
[18] B. Audiard, I. Thery-Parisot, T. Blasco, C. Mologni, P.-J. Texier, G. Battipaglia, Crossing taxonomic and isotopic approaches in charcoal analyses to reveal past climates. New perspectives in Paleobotany from the Paleolithic Neanderthal dwelling-site of La Combette (Vaucluse, France), Rev. Palaeobot. Palynol. 266 (2019) 52–60. https://doi.org/10.1016/j.revpalbo.2019.04.002.
[19] C. Di Blasi, Modeling chemical and physical processes of wood and biomass pyrolysis, Prog. Energy Combust. Sci. 34 (2008) 47–90. https://doi.org/10.1016/j.pecs.2006.12.001.
[20] G. Li, L. Gao, F. Liu, M. Qiu, G. Dong, Quantitative studies on charcoalification: Physical and chemical changes of charring wood, Fundam. Res. (2022). https://doi.org/10.1016/j.fmre.2022.05.014.

[21] F. Braadbaart, I. Poole, Morphological, chemical and physical changes during charcoalification of wood and its relevance to archaeological contexts, J. Archaeol. Sci. 35 (2008) 2434–2445. https://doi.org/10.1016/j.jas.2008.03.016.
[22] L.A. Pyle, W.C. Hockaday, T. Boutton, K. Zygourakis, T.J. Kinney, C.A. Masiello, Chemical and Isotopic Thresholds in Charring: Implications for the Interpretation of Charcoal Mass and Isotopic Data, Environ. Sci. Technol. 49 (2015) 14057–14064. https://doi.org/10.1021/acs.est.5b03087.
[23] C.I. Czimczik, C.M. Preston, M.W.I. Schmidt, R.A. Werner, E.-D. Schulze, Effects of charring on mass, organic carbon, and stable carbon isotope composition of wood, Org. Geochem. 33 (2002) 1207–1223. https://doi.org/10.1016/S0146-6380(02)00137-7.
[24] A.V. McBeath, R.J. Smernik, M.P.W. Schneider, M.W.I. Schmidt, E.L. Plant, Determination of the aromaticity and the degree of aromatic condensation of a thermosequence of wood charcoal using NMR, Org. Geochem. 42 (2011) 1194–1202. https://doi.org/10.1016/j.orggeochem.2011.08.008.
[25] S. Chatterjee, F. Santos, S. Abiven, B. Itin, R.E. Stark, J.A. Bird, Elucidating the chemical structure of pyrogenic organic matter by combining magnetic resonance, mid-infrared spectroscopy and mass spectrometry, Org. Geochem. 51 (2012) 35–44. https://doi.org/10.1016/j.orggeochem.2012.07.006.
[26] M.I. Bird, P.L. Ascough, Isotopes in pyrogenic carbon: A review, Org. Geochem. 42 (2012) 1529–1539. https://doi.org/10.1016/j.orggeochem.2010.09.005.
[27] D.B. Wiedemeier, S. Abiven, W.C. Hockaday, M. Keiluweit, M. Kleber, C.A. Masiello, A.V. McBeath, P.S. Nico, L.A. Pyle, M.P.W. Schneider, R.J. Smernik, G.L.B. Wiesenberg, M.W.I. Schmidt, Aromaticity and degree of aromatic condensation of char, Org. Geochem. 78 (2015) 135–143. https://doi.org/10.1016/j.orggeochem.2014.10.002.
[28] W.D. Gosling, H.L. Cornelissen, C.N.H. McMichael, Reconstructing past fire temperatures from ancient charcoal material, Palaeogeogr. Palaeoclimatol. Palaeoecol. 520 (2019) 128–137. https://doi.org/10.1016/j.palaeo.2019.01.029.
[29] H. Hercman, M. Szczerba, P. Zawidzki, A. Trojan, Carbon isotopes in wood combustion/pyrolysis products: experimental and molecular simulation approaches, Geochronometria. 46 (2019) 111–124. https://doi.org/10.1515/geochr-2015-0110.
[30] H. Yang, R. Yan, H. Chen, D.H. Lee, C. Zheng, Characteristics of hemicellulose, cellulose and lignin pyrolysis, Fuel. 86 (2007) 1781–1788. https://doi.org/10.1016/j.fuel.2006.12.013.
[31] J. Tintner, C. Preimesberger, C. Pfeifer, D. Soldo, F. Ottner, K. Wriessnig, H. Rennhofer, H. Lichtenegger, E.H. Novotny, E. Smidt, Impact of Pyrolysis Temperature on Charcoal Characteristics, Ind. Eng. Chem. Res. 57 (2018) 15613–15619. https://doi.org/10.1021/acs.iecr.8b04094.
[32] J. Gray, P. Thompson, Climatic information from 18O/16O analysis of cellulose, lignin and whole wood from tree rings, Nature. 270 (1977) 708–709. https://doi.org/10.1038/270708a0.
[33] J.P. Ferrio, J. Voltas, Carbon and oxygen isotope ratios in wood constituents of Pinus halepensis as indicators of precipitation, temperature and vapour pressure deficit, Tellus B Chem. Phys. Meteorol. 57 (2005) 164–173. https://doi.org/10.3402/tellusb.v57i2.16780.
[34] C.S.M. Turney, D. Wheeler, A.R. Chivas, Carbon isotope fractionation in wood during carbonization, Geochim. Cosmochim. Acta. 70 (2006) 960–964. https://doi.org/10.1016/j.gca.2005.10.031.
[35] C. Mouraux, F. Delarue, J. Bardin, T.T. Nguyen Tu, L. Bellot-Gurlet, C. Paris, S. Coubray, A. Dufraisse, Assessing the carbonisation temperatures recorded by ancient

charcoals for δ13C-based palaeoclimate reconstruction, Sci. Rep. 12 (2022) 14662. https://doi.org/10.1038/s41598-022-17836-2.
[36] P.L. Ascough, M.I. Bird, P. Wormald, C.E. Snape, D. Apperley, Influence of production variables and starting material on charcoal stable isotopic and molecular characteristics, Geochim. Cosmochim. Acta. 72 (2008) 6090–6102. https://doi.org/10.1016/j.gca.2008.10.009.
[37] P.-J. Hatton, S. Chatterjee, T.R. Filley, K. Dastmalchi, A.F. Plante, S. Abiven, X. Gao, C.A. Masiello, S.W. Leavitt, K.J. Nadelhoffer, R.E. Stark, J.A. Bird, Tree taxa and pyrolysis temperature interact to control the efficacy of pyrogenic organic matter formation, Biogeochemistry. 130 (2016) 103–116. https://doi.org/10.1007/s10533-016-0245-1.
[38] M.W. Hamilton, Reconstructing Fire Severity From the Oxygen-Isotope Compositions of Plant Char, (2012) 130.
[39] F. Behar, V. Beaumont, H.L. De B. Penteado, Rock-Eval 6 Technology: Performances and Developments, Oil Gas Sci. Technol. 56 (2001) 111–134. https://doi.org/10.2516/ogst:2001013.
[40] T. Boettger, M. Haupt, K. Knöller, S.M. Weise, J.S. Waterhouse, K.T. Rinne, N.J. Loader, E. Sonninen, H. Jungner, V. Masson-Delmotte, M. Stievenard, M.-T. Guillemin, M. Pierre, A. Pazdur, M. Leuenberger, M. Filot, M. Saurer, C.E. Reynolds, G. Helle, G.H. Schleser, Wood Cellulose Preparation Methods and Mass Spectrometric Analyses of δ13C, δ18O, and Nonexchangeable δ2H Values in Cellulose, Sugar, and Starch: An Interlaboratory Comparison, Anal. Chem. 79 (2007) 4603–4612. https://doi.org/10.1021/ac0700023.
[41] Van Krevelen, Graphical-statistical method for the study of structure and reaction processes of coal, Fuel. (1950) 269–284.
[42] K. Hammes, R.J. Smernik, J.O. Skjemstad, A. Herzog, U.F. Vogt, M.W.I. Schmidt, Synthesis and characterisation of laboratory-charred grass straw (Oryza sativa) and chestnut wood (Castanea sativa) as reference materials for black carbon quantification, Org. Geochem. 37 (2006) 1629–1633. https://doi.org/10.1016/j.orggeochem.2006.07.003.
[43] Y. Guo, R.M. Bustin, FTIR spectroscopy and reflectance of modern charcoals and fungal decayed woods: implications for studies of inertinite in coals, Int. J. Coal Geol. 37 (1998) 29–53. https://doi.org/10.1016/S0166-5162(98)00019-6.
[44] B. Esteves, A. Velez Marques, I. Domingos, H. Pereira, Chemical changes of heat treated pine and eucalypt wood monitored by FTIR, Maderas Cienc. Tecnol. 15 (2013) 245–258. https://doi.org/10.4067/S0718-221X2013005000020.
[45] K. Ishimaru, T. Hata, P. Bronsveld, D. Meier, Y. Imamura, Spectroscopic analysis of carbonization behavior of wood, cellulose and lignin, J. Mater. Sci. 42 (2007) 122–129. https://doi.org/10.1007/s10853-006-1042-3.
[46] J. Yu, L. Sun, C. Berrueco, B. Fidalgo, N. Paterson, M. Millan, Influence of temperature and particle size on structural characteristics of chars from Beechwood pyrolysis, J. Anal. Appl. Pyrolysis. 130 (2018) 127–134. https://doi.org/10.1016/j.jaap.2018.01.018.
[47] J. Lehto, J. Louhelainen, T. Kłosińska, M. Drożdżek, R. Alén, Characterization of alkali-extracted wood by FTIR-ATR spectroscopy, Biomass Convers. Biorefinery. 8 (2018) 847–855. https://doi.org/10.1007/s13399-018-0327-5.
[48] O. Gonultas, Z. Candan, O. Gonultas, Z. Candan, Chemical characterization and ftir spectroscopy of thermally compressed eucalyptus wood panels, Maderas Cienc. Tecnol. 20 (2018) 431–442. https://doi.org/10.4067/S0718-221X2018005031301.

[49] S.-M. Kwon, J.-H. Jang, S.-H. Lee, S.-B. Park, N.-H. Kim, Change of Heating Value, pH and FT-IR Spectra of Charcoal at Different Carbonization Temperatures, J. Korean Wood Sci. Technol. 41 (2013) 440–446. https://doi.org/10.5658/WOOD.2013.41.5.440.
[50] S. Cheng, A. Huang, S. Wang, Q. Zhang, Effect of Different Heat Treatment Temperatures on the Chemical Composition and Structure of Chinese Fir Wood, BioResources. 11 (2016) 4006–4016.
[51] M. Müller-Hagedorn, H. Bockhorn, L. Krebs, U. Müller, A comparative kinetic study on the pyrolysis of three different wood species, J. Anal. Appl. Pyrolysis. 68–69 (2003) 231–249. https://doi.org/10.1016/S0165-2370(03)00065-2.
[52] M. Zech, R.A. Werner, D. Juchelka, K. Kalbitz, B. Buggle, B. Glaser, Absence of oxygen isotope fractionation/exchange of (hemi-) cellulose derived sugars during litter decomposition, Org. Geochem. 42 (2012) 1470–1475. https://doi.org/10.1016/j.orggeochem.2011.06.006.
[53] H.-L. Schmidt, R.A. Werner, A. Roßmann, 18O Pattern and biosynthesis of natural plant products, Phytochemistry. 58 (2001) 9–32. https://doi.org/10.1016/S0031-9422(01)00017-6.
[54] F.-X. Collard, J. Blin, A review on pyrolysis of biomass constituents: Mechanisms and composition of the products obtained from the conversion of cellulose, hemicelluloses and lignin, Renew. Sustain. Energy Rev. 38 (2014) 594–608. https://doi.org/10.1016/j.rser.2014.06.013.
[55] C. Li, Y. Sun, L. Zhang, Q. Li, S. Zhang, X. Hu, Sequential pyrolysis of coal and biomass: Influence of coal-derived volatiles on property of biochar, Appl. Energy Combust. Sci. 9 (2022) 100052. https://doi.org/10.1016/j.jaecs.2021.100052.
[56] W.-H. Chen, C.-W. Wang, H.C. Ong, P.L. Show, T.-H. Hsieh, Torrefaction, pyrolysis and two-stage thermodegradation of hemicellulose, cellulose and lignin, Fuel. 258 (2019) 116168. https://doi.org/10.1016/j.fuel.2019.116168.
[57] R. Benner, M.L. Fogel, E.K. Sprague, R.E. Hodson, Depletion of 13C in lignin and its implications for stable carbon isotope studies, Nature. 329 (1987) 708–710. https://doi.org/10.1038/329708a0.
[58] N.J. Loader, I. Robertson, D. McCarroll, Comparison of stable carbon isotope ratios in the whole wood, cellulose and lignin of oak tree-rings, Palaeogeogr. Palaeoclimatol. Palaeoecol. 196 (2003) 395–407. https://doi.org/10.1016/S0031-0182(03)00466-8.
[59] V.C. Turekian, S. Macko, D. Ballentine, R.J. Swap, M. Garstang, Causes of bulk carbon and nitrogen isotopic fractionations in the products of vegetation burns: laboratory studies, Chem. Geol. 152 (1998) 181–192. https://doi.org/10.1016/S0009-2541(98)00105-3.
[60] E. Leng, Y. Guo, J. Chen, S. Liu, J. E, Y. Xue, A comprehensive review on lignin pyrolysis: Mechanism, modeling and the effects of inherent metals in biomass, Fuel. 309 (2022) 122102. https://doi.org/10.1016/j.fuel.2021.122102.
[61] Q. Liu, S. Wang, Y. Zheng, Z. Luo, K. Cen, Mechanism study of wood lignin pyrolysis by using TG–FTIR analysis, J. Anal. Appl. Pyrolysis. 82 (2008) 170–177. https://doi.org/10.1016/j.jaap.2008.03.007.
[62] G. Fronza, C. Fuganti, S. Serra, A. Burke, C. Guillou, F. Reniero, The Positional δ(18O) Values of Extracted and Synthetic Vanillin, Helv. Chim. Acta. 84 (2001) 351–359. https://doi.org/10.1002/1522-2675(20010228)84:2<351::AID-HLCA351>3.0.CO;2-S.
[63] X. Cao, J.J. Pignatello, Y. Li, C. Lattao, M.A. Chappell, N. Chen, L.F. Miller, J. Mao, Characterization of Wood Chars Produced at Different Temperatures Using Advanced Solid-State 13C NMR Spectroscopic Techniques, Energy Fuels. 26 (2012) 5983–5991. https://doi.org/10.1021/ef300947s.

[64] R.K. Sharma, J.B. Wooten, V.L. Baliga, X. Lin, W. Geoffrey Chan, M.R. Hajaligol, Characterization of chars from pyrolysis of lignin, Fuel. 83 (2004) 1469–1482. https://doi.org/10.1016/j.fuel.2003.11.015.
[65] G. Lévy, C. Bréchet, M. Becker, Element analysis of tree rings in pedunculate oak heartwood: an indicator of historical trends in the soil chemistry, related to atmospheric deposition, Ann. Sci. For. 53 (1996) 685–696. https://doi.org/10.1051/forest:19960246.
[66] V. Penninckx, S. Glineur, W. Gruber, J. Herbauts, P. Meerts, Radial variations in wood mineral element concentrations: a comparison of beech and pedunculate oak from the Belgian Ardennes, Ann. For. Sci. 58 (2001) 253–260. https://doi.org/10.1051/forest:2001124.
[67] F. André, M. Jonard, Q. Ponette, Biomass and nutrient content of sessile oak (Quercus petraea (Matt.) Liebl.) and beech (Fagus sylvatica L.) stem and branches in a mixed stand in southern Belgium, Sci. Total Environ. 408 (2010) 2285–2294. https://doi.org/10.1016/j.scitotenv.2010.02.040.
[68] D. Vansteenkiste, J. Van Acker, M. Stevens, D. Le Thiec, G. Nepveu, Composition, distribution and supposed origin of mineral inclusions in sessile oak wood — consequences for microdensitometrical analysis, Ann. For. Sci. 64 (2007) 11–19. https://doi.org/10.1051/forest:2006083.
[69] A.I. Štulc, A. Poszwa, S. Ponton, J.-L. Dupouey, J. Bouchez, J. Bardin, F. Delarue, S. Coubray, M. Lemoine, C. Rose, J. Ruelle, M. Beuret, T.T.N. Tu, A. Dufraisse, Multi-elemental and Strontium-Neodymium Isotopic Signatures in Charred Wood: Potential for Wood Provenance Studies, Int. J. Wood Cult. 1 (2023) 1–48. https://doi.org/10.1163/27723194-bja10019.
[70] S. Carlquist, Cell Contents, Secretory Structures, in: S. Carlquist (Ed.), Comp. Wood Anat. Syst. Ecol. Evol. Asp. Dicotyledon Wood, Springer, Berlin, Heidelberg, 2001: pp. 229–270. https://doi.org/10.1007/978-3-662-04578-7_7.
[71] D.J. Nowakowski, J.M. Jones, Uncatalysed and potassium-catalysed pyrolysis of the cell-wall constituents of biomass and their model compounds, J. Anal. Appl. Pyrolysis. 83 (2008) 12–25. https://doi.org/10.1016/j.jaap.2008.05.007.
[72] I.-Y. Eom, J.-Y. Kim, T.-S. Kim, S.-M. Lee, D. Choi, I.-G. Choi, J.-W. Choi, Effect of essential inorganic metals on primary thermal degradation of lignocellulosic biomass, Bioresour. Technol. 104 (2012) 687–694. https://doi.org/10.1016/j.biortech.2011.10.035.
[73] F. Rees, F. Watteau, S. Mathieu, M.-P. Turpault, Y. Le Brech, R. Qiu, J.L. Morel, Metal Immobilization on Wood-Derived Biochars: Distribution and Reactivity of Carbonate Phases, J. Environ. Qual. 46 (2017) 845–854. https://doi.org/10.2134/jeq2017.04.0152.
[74] W.A. Brand, T.B. Coplen, J. Vogl, M. Rosner, T. Prohaska, Assessment of international reference materials for isotope-ratio analysis (IUPAC Technical Report), Pure Appl. Chem. 86 (2014) 425–467. https://doi.org/10.1515/pac-2013-1023.
[75] M. Schumacher, R. Werner, H.A.J. Meijer, H. Jansen, W. Brand, H. Geilmann, R. Neubert, Oxygen isotopic signature of CO2 from combustion processes, Atmospheric Chem. Phys. (2011). https://doi.org/10.5194/acp-11-1473-2011.
[76] C. Santín, S.H. Doerr, A. Merino, T.D. Bucheli, R. Bryant, P. Ascough, X. Gao, C.A. Masiello, Carbon sequestration potential and physicochemical properties differ between wildfire charcoals and slow-pyrolysis biochars, Sci. Rep. 7 (2017) 11233. https://doi.org/10.1038/s41598-017-10455-2.
[77] M.P.W. Schneider, L.A. Pyle, K.L. Clark, W.C. Hockaday, C.A. Masiello, M.W.I. Schmidt, Toward a "Molecular Thermometer" to Estimate the Charring Temperature of Wildland Charcoals Derived from Different Biomass Sources, ACS Publ. (2013). https://doi.org/10.1021/es401430f.

[78] K.A. Spokas, Review of the stability of biochar in soils: predictability of O:C molar ratios, Carbon Manag. 1 (2010) 289–303. https://doi.org/10.4155/cmt.10.32.
[79] M.X. Fang, D.K. Shen, Y.X. Li, C.J. Yu, Z.Y. Luo, K.F. Cen, Kinetic study on pyrolysis and combustion of wood under different oxygen concentrations by using TG-FTIR analysis, J. Anal. Appl. Pyrolysis. 77 (2006) 22–27. https://doi.org/10.1016/j.jaap.2005.12.010.
[80] V. Sarangi, S. Roy, P. Sanyal, Effect of burning on the distribution pattern and isotopic composition of plant biomolecules: Implications for paleoecological studies, Geochim. Cosmochim. Acta. 318 (2022) 305–327. https://doi.org/10.1016/j.gca.2021.12.003.
[81] Y. Yang, T. Fu, F. Song, X. Song, X.-L. Wang, Y.-Z. Wang, Wood-burning processes in variable oxygen atmospheres: Thermolysis, fire, and smoke release behavior, Polym. Degrad. Stab. 205 (2022) 110158. https://doi.org/10.1016/j.polymdegradstab.2022.110158.
[82] C. Chen, L. Zhao, J. Wang, S. Lin, Reactive Molecular Dynamics Simulations of Biomass Pyrolysis and Combustion under Various Oxidative and Humidity Environments, Ind. Eng. Chem. Res. 56 (2017) 12276–12288. https://doi.org/10.1021/acs.iecr.7b01714.
[83] K. Cheng, W.T. Winter, A.J. Stipanovic, A modulated-TGA approach to the kinetics of lignocellulosic biomass pyrolysis/combustion, Polym. Degrad. Stab. 97 (2012) 1606–1615. https://doi.org/10.1016/j.polymdegradstab.2012.06.027.
[84] R. Vernooij, U. Dusek, M.E. Popa, P. Yao, A. Shaikat, C. Qiu, P. Winiger, C. van der Veen, T.C. Eames, N. Ribeiro, G.R. van der Werf, Stable carbon isotopic composition of biomass burning emissions – implications for estimating the contribution of C_3 and C_4 plants, Atmospheric Chem. Phys. 22 (2022) 2871–2890. https://doi.org/10.5194/acp-22-2871-2022.
[85] J. Li, B. Li, X. Zhang, Comparative studies of thermal degradation between larch lignin and manchurian ash lignin, Polym. Degrad. Stab. 78 (2002) 279–285. https://doi.org/10.1016/S0141-3910(02)00172-6.
[86] X. Xiao, Z. Chen, B. Chen, H/C atomic ratio as a smart linkage between pyrolytic temperatures, aromatic clusters and sorption properties of biochars derived from diverse precursory materials, Sci. Rep. 6 (2016) 22644. https://doi.org/10.1038/srep22644.
[87] N.J. Loader, P.M. Santillo, J.P. Woodman-Ralph, J.E. Rolfe, M.A. Hall, M. Gagen, I. Robertson, R. Wilson, C.A. Froyd, D. McCarroll, Multiple stable isotopes from oak trees in southwestern Scotland and the potential for stable isotope dendroclimatology in maritime climatic regions, Chem. Geol. 252 (2008) 62–71. https://doi.org/10.1016/j.chemgeo.2008.01.006.
[88] K.T. Rinne, N.J. Loader, V.R. Switsur, J.S. Waterhouse, 400-year May–August precipitation reconstruction for Southern England using oxygen isotopes in tree rings, Quat. Sci. Rev. 60 (2013) 13–25. https://doi.org/10.1016/j.quascirev.2012.10.048.
[89] I. Labuhn, V. Daux, O. Girardclos, M. Stievenard, M. Pierre, V. Masson-Delmotte, French summer droughts since 1326 CE: a reconstruction based on tree ring cellulose $\delta^{18}O$, Clim. Past. 12 (2016) 1101–1117. https://doi.org/10.5194/cp-12-1101-2016.
[90] V. Daux, A. Michelot-Antalik, A. Lavergne, M. Pierre, M. Stievenard, N. Bréda, C. Damesin, Comparisons of the Performance of $\delta^{13}C$ and $\delta^{18}O$ of *Fagus sylvatica* , *Pinus sylvestris* , and *Quercus petraea* in the Record of Past Climate Variations, J. Geophys. Res. Biogeosciences. 123 (2018) 1145–1160. https://doi.org/10.1002/2017JG004203.
[91] I. Cohen-Ofri, L. Weiner, E. Boaretto, G. Mintz, S. Weiner, Modern and fossil charcoal: aspects of structure and diagenesis, J. Archaeol. Sci. 33 (2006) 428–439. https://doi.org/10.1016/j.jas.2005.08.008.

[92] P.L. Ascough, M.I. Bird, A.C. Scott, M.E. Collinson, I. Cohen-Ofri, C.E. Snape, K. Le Manquais, Charcoal reflectance measurements: implications for structural characterization and assessment of diagenetic alteration, J. Archaeol. Sci. 37 (2010) 1590–1599. https://doi.org/10.1016/j.jas.2010.01.020.